PHYSICAL REVIEW B VOLUME 35, NUMBER 8 15 MARCH 1987-I

Photoemission, inverse photoemission, and fluctuations in an exactly soluble many-body cluster model of bcc iron

Erik C. Sowa and L. M. Falicov
Department of Physics, University of California, Berkeley, California 94720
and Materials and Molecular Research Division, Lawrence Berkeley Laboratory, University of California, Berkeley, California 94720
(Received 6 October 1986)

An exact solution for a two-site crystal model, the smallest body-centered-cubic crystal, is presented for iron. The model consists of five d-like orbitals per site per spin, with interatomic hopping terms and an on-site Coulomb interaction of the fullest generality allowed by atomic symmetry. The ground state, depending on the choice of one-electron parameters, is found in one case to be a fully saturated ferromagnet, and in another to be an unsaturated ferromagnet with strong antiferromagnetic fluctuations. The many-body energy-level spectrum, intracluster charge and spin fluctuations, and photoemission and inverse photoemission densities of states for both cases are calculated and compared with experiment.

I. INTRODUCTION

Electrons in the d shell are responsible for many of the interesting properties of transition metals. In particular, the magnetism of Fe, Co, and Ni derives from the Coulomb interaction between electrons in an unfilled d shell, or an unfilled d band in the case of a periodic solid. In fact, the d-band width and the intra-atomic Coulomb interaction are of comparable magnitude in these metals.

As a consequence of the competition between band-structure effects (manifested in the d-band width) and the Coulomb interaction, there are two different ways to analyze electronic phenomena in these metals. An itinerant or band description of the $3d$ electrons is useful for the interpretation of de Haas–van Alphen effect, magnetotransport, and photoemission experiments, whereas a localized-moment picture is more compatible with the Curie-type behavior of the susceptibility, with the existence of spin waves above T_c, and with the magnetic form factors.[1] Neither point of view is complete. The success of both pictures serves to emphasize that the determination of the electronic structure of these metals is a full many-body problem, and that even delocalized d electrons are strongly correlated.

The huge number of particles in a macroscopic crystal makes the solution of the full many-body problem in such a system intractable. The traditional way around this dilemma takes the one-particle picture as basic and includes many-body effects only in the form of a suitably averaged single-particle exchange-correlation potential. This approach has been very successful in explaining properties of both bulk crystals[2–6] and clusters.[7,8] One can, however, find exceptions to this general pattern of success. These exceptions typically involve many-body effects that cannot be taken into account by this sort of averaging. Perhaps the most famous example of this is the valence-band photoemission satellite[9] approximately 6 eV below the Fermi level in fcc Ni. Much theoretical attention[10] has been focused on this feature, as well as other many-body corrections to the Ni density of emitted states; one successful treatment by Victora and Falicov[11] uses a recently developed finite-cluster method.[12–14]

The finite-cluster method is a full many-body approach which reduces the size of the problem from a macroscopic to a limited-size crystal, while maintaining periodic boundary conditions in order to eliminate surface effects. In this way, one can explicitly include band-structure effects and the Coulomb interaction in a model Hamiltonian small enough that the many-body eigenstates and energies can be obtained by straightforward diagonalization. The results are exact within the context of the model Hamiltonian. Because of the small size of the crystal (Victora and Falicov used a four-atom tetrahedral cluster to model fcc Ni), one would not expect this method to yield accurate long-range correlations or sharp phase transitions; however, uniform properties and short-range correlations should be well represented. This accounts for the method's success in treating the photoemission problem.

In this paper, this method is applied to bcc Fe. Iron is an interesting case because it has more d holes per atom than Ni, as well as a different crystal structure; it is also the prototypical ferromagnet. It is found in this case that the method models a "weak" ferromagnet in the sense that a small change in one of the one-particle parameters of the Hamiltonian causes the many-body ground state to change from a saturated (fully spin-polarized) ferromagnet to an unsaturated ferromagnet with strong antiferromagnetic fluctuations. Section II is a detailed description of the model. Section III contains our analysis of the many-body eigenvalue spectrum, and Sec. IV shows the one-particle densities of states that would be measured in photoemission and inverse photoemission experiments. The results are summarized in Sec. V.

II. THE MODEL HAMILTONIAN

The smallest nontrivial bcc crystal contains two atoms. With periodic boundary conditions, a calculation using this crystal is equivalent to a restricted sampling of two

TABLE I. Hamiltonian parameters (units of rydbergs).

	Unsaturated ferromagnet	Saturated ferromagnet
$(dd\sigma)_1$	−0.056 69	−0.056 69
$(dd\pi)_1$	0.037 38	0.037 38
$(dd\delta)_1$	−0.006 69	−0.006 69
$(dd\sigma)_2$	−0.033 67	−0.033 67
$(dd\pi)_2$	0.010 00	0.010 00
$(dd\delta)_2$	−0.000 75	−0.000 75
e_3	0.747 75	0.789 99
e_5	0.768 99	0.768 99
γ_3	0.8260	0.8683
γ_5	0.6990	0.6990
h_3	0.4630	0.5052
h_5	0.9160	0.9160
U	0.3600	0.3600
J	0.0514	0.0514
ΔJ	0.0064	0.0064

points in the Brillouin zone. These two points, both of which have full cubic symmetry, are Γ (the zone center) and H (the point at the end of the cubic axes). There are five d orbitals per atom per spin; in the presence of a cubic field they split into the triplet t_{2g} and the doublet e_g.

The model Hamiltonian contains both single-particle and two-particle terms:

$$H=\sum_{i\neq j;\mu,\nu;\sigma} t_{i\mu,j\nu}c^{\dagger}_{i\mu\sigma}c_{j\nu\sigma}+\sum_{i;\mu;\sigma} e_{\mu}c^{\dagger}_{i\mu\sigma}c_{i\mu\sigma} + \sum_{i;\mu,\nu,\lambda,\phi;\sigma,\sigma'} V_{\mu\nu\lambda\phi}c^{\dagger}_{i\mu\sigma}c^{\dagger}_{i\nu\sigma'}c_{i\lambda\sigma'}c_{i\phi\sigma} \ . \quad (2.1)$$

Here i,j $(=1,2)$ label atoms, μ,ν,λ,ϕ label orbitals, and σ,σ' label spins. The single-particle hopping terms $t_{i\mu,j\nu}$ are parametrized according to the Slater-Koster tight-binding scheme.[15] Note that this scheme allows for only nearest-neighbor hopping; in our restricted crystal the second nearest neighbor of an atom is itself. Intra-atomic Coulomb interactions $V_{\mu\nu\lambda\phi}$ are used; they include a direct Coulomb integral U, an average exchange integral

$$J=\tfrac{1}{2}[J(e_g,e_g)+J(t_{2g},t_{2g})] \ ,$$

and an exchange anisotropy

$$\Delta J=[J(e_g,e_g)-J(t_{2g},t_{2g})] \ .$$

Following Victora and Falicov,[11] a value for U is chosen and the other interaction parameters are set in the ratios $U:J:\Delta J=56:8:1$. (The results are insensitive to the exact values of these ratios.) The next largest contribution is the nearest-neighbor Coulomb term, which makes a constant contribution and may be neglected.

Two different sets of Slater-Koster parameters are used. The first set is chosen to reproduce, in the absence of any interactions, the calculated paramagnetic local-density approximation (LDA) band structure of Moruzzi *et al.*[16] at the Γ and H points. In order to accomplish this, it is necessary to assign different values to the occupation energies e_3 and e_5 of the e_g and the t_{2g} bands, respectively.[17] This relative shift is caused by hybridization between the d bands and the sp bands, as well as second-neighbor hopping between the atoms. The second set differs from the first only in the value of the shift; in the set that reproduces the LDA result, the occupation energies satisfy $e_5-e_3=0.29$ eV, while in the other set $e_5-e_3=-0.29$ eV. The value[18] for U, which is used with both one-particle parameter sets, is 4.9 eV, considerably larger than the Hartree-Fock value.[19] Such a large value is necessary because the screening of U is explicitly included in this treatment. The parameters are summarized in Table I.

Since metallic Fe has a magnetic moment of $2.22\mu_B$ per atom,[20] and the method allows only an integral number of particles in the cluster, the configuration chosen is four d holes in the neutral state of the cluster. In this configuration there is an average of two holes per atom; therefore the maximum possible magnetic moment per atom is $2.00\mu_B$. Simple combinatorial arguments yield 4845 states for this number of holes. The photoemission process adds a fifth hole, yielding 15 504 final states. Inverse

TABLE II. Two-atom bcc space-group character table (inversion omitted).

		1 E	3 C_4^2	6 C_4	6 C_2	8 C_3	1 τ^a	3 τC_4^2	6 τC_4	6 τC_2	8 τC_3
s	Γ_1	1	1	1	1	1	1	1	1	1	1
	Γ_2	1	1	−1	−1	1	1	1	−1	−1	1
e_g	Γ_3	2	2	0	0	−1	2	2	0	0	−1
p	Γ_4	3	−1	1	−1	0	3	−1	1	−1	0
t_{2g}	Γ_5	3	−1	−1	1	0	3	−1	−1	1	0
s	H_1	1	1	1	1	1	−1	−1	−1	−1	−1
	H_2	1	1	−1	−1	1	−1	−1	1	1	−1
e_g	H_3	2	2	0	0	−1	−2	−2	0	0	1
p	H_4	3	−1	1	−1	0	−3	1	−1	1	0
t_{2g}	H_5	3	−1	−1	1	0	−3	1	1	−1	0

[a]The symbol τ stands for the operation that translates from one lattice site to the other.

TABLE III. Sizes of blocks of the various representations.

N	Spin	Γ_1	Γ_2	Γ_3	Γ_4	Γ_5	H_1	H_2	H_3	H_4	H_5
3	$\frac{3}{2}$	1	3	4	9	7	1	3	4	9	7
	$\frac{1}{2}$	6	6	15	20	21	6	6	15	20	21
4	2	6	4	11	11	15	2	4	8	14	12
	1	16	22	37	67	59	20	22	40	64	62
	0	29	16	40	44	56	18	18	32	50	50
5	$\frac{5}{2}$	9	5	11	14	16	9	5	11	14	16
	$\frac{3}{2}$	37	39	76	117	115	37	39	76	117	115
	$\frac{1}{2}$	71	67	141	202	208	71	67	141	202	208

photoemission removes a hole, leaving three in the cluster for a total of 1140 final states.

Clearly, even the two-atom cluster model for Fe has a very large Hamiltonian. The symmetries inherent in the Hamiltonian (2.1) must be exploited to reduce further the size of the matrices to be diagonalized.

The space group of the two-atom bcc lattice contains 96 operations including the inversion i. The point group is $O_h = O \times i$. Since only d orbitals are included, and they are even under i, the inversion operation may be ignored. A restricted set of 48 operations, with 10 irreducible representations (5 each at Γ and H), is sufficient. The representations are shown in Table II, the character table of the space group. With a complete set of matrices that transform according to these irreducible representations,[21] it is possible to project out sets of symmetrized basis states. Since the representations cannot mix, this is equivalent to a block diagonalization of the Hamiltonian. In the case of 5 holes in the cluster the largest block is 339×339, a considerable reduction from the original $15\,504 \times 15\,504$ matrix.

The symmetry of the Hamiltonian also requires that the eigenstates have definite spin angular momentum. This symmetry may also be exploited for further block diagonalization; the sizes of the reduced blocks for 3, 4, and 5 holes are shown in Table III. Of course, the solutions obtained by diagonalizing these blocks are exact solutions of the full Hamiltonian for the cluster.

III. EIGENVALUE SPECTRUM AND THERMODYNAMICS

The neutral state contains $N = 4$ holes in the cluster. It admits spin singlets, triplets, and quintets. The quintets represent saturated ferromagnetic solutions, the triplets represent unsaturated ferromagnets (possibly though not necessarily ferromagnetic states), and the singlets could be paramagnets or antiferromagnets. Two states lie below all others: one is of ${}^3\Gamma_4$ symmetry, the other is ${}^5H_3$. With the first set of Slater-Koster parameters, the unsaturated ferromagnet ${}^3\Gamma_4$ is the ground state; with the second set, the saturated ferromagnet ${}^5H_3$ is lower. Both are spatially degenerate representations. The unsaturated ferromagnet is spatially uniform; the saturated ferromagnet changes phase with the nearest-neighbor translation operation. In both cases, the two states are very close to one another in energy. The reason that the first set does not yield a saturated ferromagnet can be understood from the following rough argument, in which lower case letters are used to denote the symmetry of the single-particle energy levels. In both cases, the highest one-electron energy level (the first to be "occupied" by holes) is h_5. It can accommodate three holes of each spin. When the Coulomb interaction is turned on, the spin states are split by approximately J. For the first set of parameters, the splitting is not sufficient to bring the h_5 majority-spin[22] level below the closest minority-spin level, which is of γ_3 symmetry. Three holes are in the minority-spin h_5 level, and the fourth hole ends up in the majority-spin h_5 level. The repulsive Coulomb interaction is not strong enough to overcome the difference in occupation energies, and the ground state is therefore not fully spin polarized. In the second case, the extra shift pushes up the e_g band so that the γ_3 level is within J range of h_5, and the fourth hole can go into the minority-spin γ_3 level. All the holes are therefore in the same spin state, and the cluster is fully spin polarized. This is, of course, only an approximate picture, since in the full many-body approach configuration interaction mixes all one-particle levels. Nevertheless, it is a useful way to understand the result, and will prove to be even more useful in the explanation of the photoemission and inverse photoemission densities of states of Sec. IV.

The density of many-body states (MB-DOS) is the best way to show the spectrum of energy eigenvalues of the Hamiltonian (2.1). At each eigenvalue,[23] a peak of weight equal to the degeneracy at that energy is plotted. In a finite system, this results in a discrete set of spikes. Spin-resolved and total MB-DOS plots for both parameter sets are shown in Figs. 1 and 2; in these figures, the spikes have been artificially broadened into Gaussians of 0.1 eV halfwidth. It is worth noting that, despite the considerable difference in ground-state properties, the densities of many-body states are remarkably similar.

The finite-cluster method can also produce the eigenstates, allowing one to compute various correlation functions. It is trivial to obtain the most obvious correlation, namely the magnitude of S^2 in the cluster. Two other functions, which require knowledge of the eigenstates, can

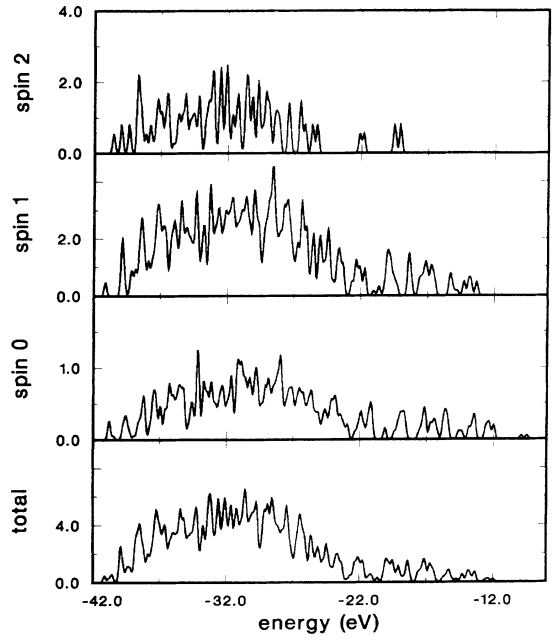

FIG. 1. Total and spin-resolved eigenvalue spectra (densities of many-body states) for the unsaturated ferromagnet.

help interpret the results. The first is

$$\Delta n^2 \equiv \left\langle \left[\sum_{\mu} (n_{1\mu\uparrow} + n_{1\mu\downarrow}) - (n_{2\mu\uparrow} + n_{2\mu\downarrow}) \right]^2 \right\rangle . \tag{3.1}$$

Here $n_{l\mu\sigma} = c^{\dagger}_{i\mu\sigma} c_{i\mu\sigma}$. The quantity Δn^2 can be called the intracluster charge fluctuation because it is simply the average of the square of the difference between the occupations of the two sites. It is a measure of the polarity of the electronic charge in the cluster; a zero value indicates a neutral cluster, while a large value indicates large charge-density fluctuations. The second function is

$$\Delta \sigma^2 \equiv \left\langle \left[\sum_{\mu} (n_{1\mu\uparrow} - n_{1\mu\downarrow}) - (n_{2\mu\uparrow} - n_{2\mu\downarrow}) \right]^2 \right\rangle , \tag{3.2}$$

which is called the intracluster spin fluctuation. It is a measure of the spin imbalance between the two sites of the cluster. A zero value indicates a uniform spin distribution, while a large value indicates large spin-density fluctuations, or equivalently antiferromagnetic correlations.

These correlations may be plotted as functions of temperature by simply calculating them for each eigenstate, multiplying by the appropriate Boltzmann factor, and adding. The thermodynamic averages of total energy, $\langle S^2 \rangle$, Δn^2, and $\Delta \sigma^2$ are shown for both parameter sets in Figs. 3 and 4. Most of the interesting behavior occurs at fairly low temperatures, because the two low-lying states are very close in energy compared to the rest of the states. The result for $\Delta \sigma^2$ is particularly interesting. Note that it is much higher for the unsaturated ferromagnet. This im-

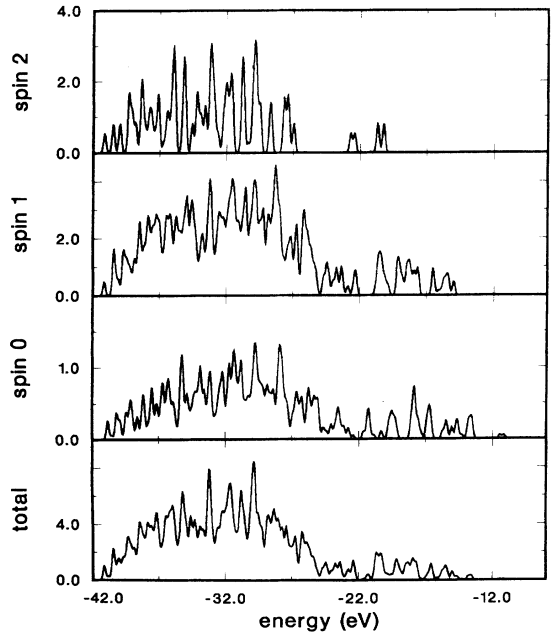

FIG. 2. Total and spin-resolved eigenvalue spectra (densities of many-body states) for the saturated ferromagnet.

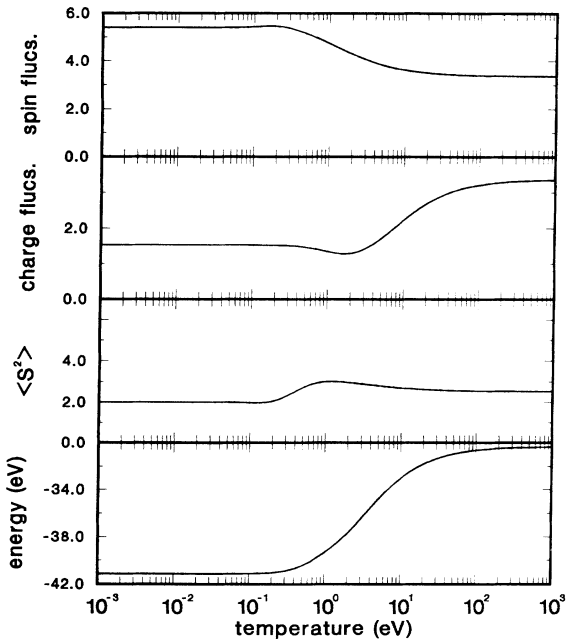

FIG. 3. Thermodynamic averages of energy, S^2, intracluster charge fluctuations, and intracluster spin fluctuations for the unsaturated ferromagnet.

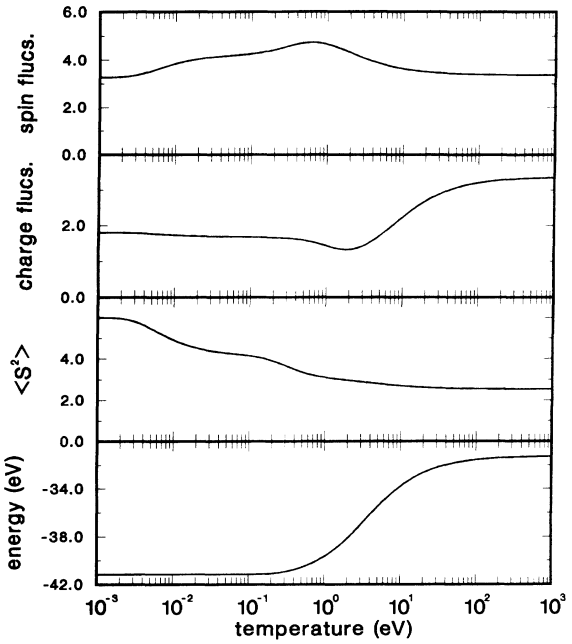

FIG. 4. Thermodynamic averages of energy, S^2, intracluster charge fluctuations, and intracluster spin fluctuations for the saturated ferromagnet.

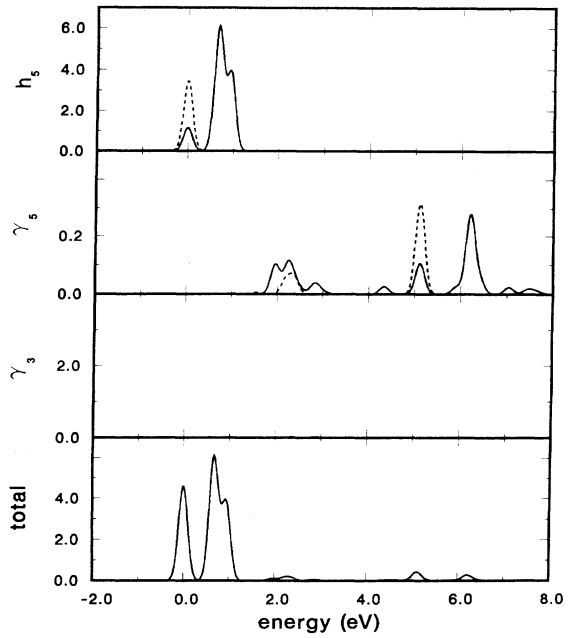

FIG. 5. Total and spin- and angle-resolved inverse photoemission densities of states for the unsaturated ferromagnet. In the spin-resolved plots, dashed and solid lines represent majority-spin and minority-spin electrons, respectively.

plies that this state has strong antiferromagnetic fluctuations, i.e., antiferromagnetic character.

IV. PHOTOEMISSION AND INVERSE PHOTOEMISSION

The photoemission process adds a fifth hole to the system. The one-electron density of (emitted) states (DOS) is calculated by adding a hole to the ground state and projecting the result onto the eigenstates of the cluster with 5 holes. When holes of particular spatial symmetry and spin orientation are added, one obtains spin- and angle-resolved densities of states. These may be added together to obtain the total d-band photoemission DOS. The inverse photoemission DOS is calculated in a similar fashion, with the annihilation of a hole from the ground state. Selected results for both sets of parameters are shown in Figs. 5 and 6. In these figures, the sharp lines characteristic of a finite system have been artificially broadened with Gaussian peaks of 0.1-eV halfwidth.

The gross features of the inverse photoemission results are easily understood with the same one-electron arguments presented in Sec. III. An electron cannot be absorbed unless there is already a hole there. According to the earlier argument, the unsaturated ground state should consist of 3 holes in minority-spin[22] levels and one in a majority-spin level, all of h_5 symmetry, and the Fermi level should be at the majority-spin energy. Indeed, the two largest peaks in the total DOS of Fig. 5 are mainly h_5, as can be seen in Fig. 5. The peak at the Fermi level

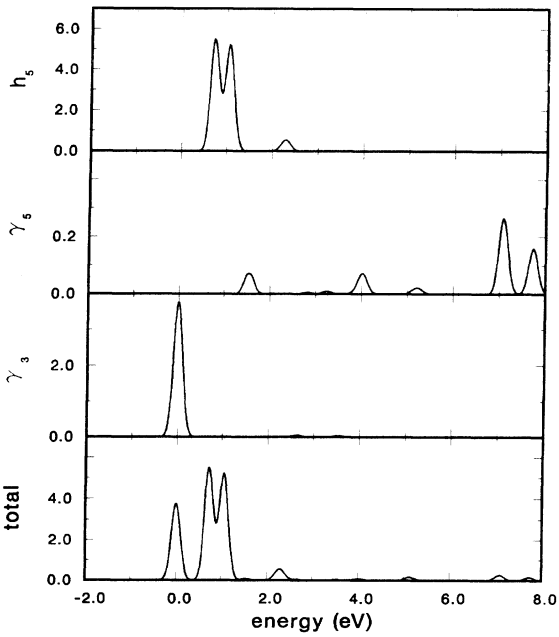

FIG. 6. Total and spin- and angle-resolved inverse photoemission densities of states for the saturated ferromagnet. In the spin-resolved plots, dashed and solid lines represent majority-spin and minority-spin electrons, respectively.

has all the majority-spin weight, with a significant amount of the minority spin mixed in. Most of the minority-spin weight is in the large peak just above the Fermi energy. The other small features above these main peaks are mostly of γ_5 symmetry. Note that γ_5 is nominally below the Fermi level; the presence of some hole character there is strictly a result of the strong electron-electron interaction. This admixture also implies that states nominally above the Fermi level may be occupied with non-negligible probability; this property could be clearly seen in the photoemission results. The saturated ground state should contain four holes in minority-spin levels, of which three are of h_5 symmetry. The fourth is γ_3, which is at the Fermi level. Indeed, there are no majority-spin lines in Fig. 6. The peak at the Fermi level is all γ_3, and the large peak just above this as well as the satellite just 2 eV above the Fermi energy can be identified as h_5. It should be clear that a spin-resolved inverse photoemission experiment could unambiguously distinguish between the two types of ground states.

If the ground state of the cluster contains four holes, it must also contain sixteen electrons. For this fundamental reason, the photoemission spectra are more complicated. Nevertheless, the gross features may still be understood with the same one-electron argument, although the finer details caused by the many-body interaction are more complicated. For the unsaturated case (Fig. 7), there is no weight coming from the minority-spin h_5 level, and the majority-spin peak of the same symmetry is at the Fermi level. In the saturated case (Fig. 8), the peak at the Fermi level is of the expected minority-spin γ_3 symmetry, with some majority-spin weight of the same symmetry mixed in by the interaction. Direct comparison to a photoemission experiment is difficult because of the coarse k-space mesh of the model. Nevertheless, qualitative agreement with experiment[24] is obtained, with the understanding that Γ stands for the half of the Brillouin zone closest to the zone center, and H stands for the other half.

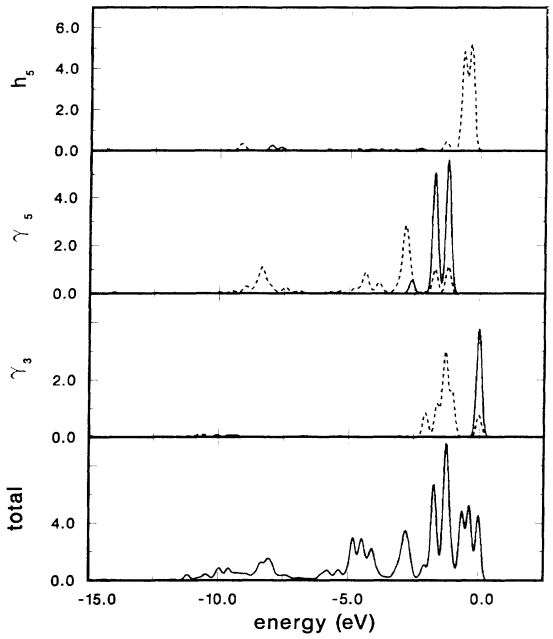

FIG. 8. Total and spin- and angle-resolved photoemission densities of states for the saturated ferromagnet. In the spin-resolved plots, dashed and solid lines represent majority-spin and minority-spin electrons, respectively.

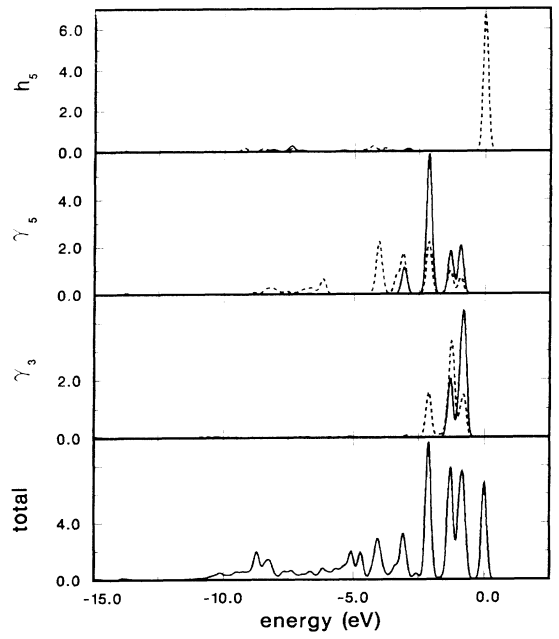

FIG. 7. Total and spin- and angle-resolved photoemission densities of states for the unsaturated ferromagnet. In the spin-resolved plots, dashed and solid lines represent majority-spin and minority-spin electrons, respectively.

For purposes of comparison, we have also computed the same densities of (photoemission and inverse photoemission) states within a single-particle (crystal-symmetry-conserving) Hartree-Fock approach. The same Hamiltonian parameters are used, with the exception that the relatively small exchange anisotropy ΔJ is ignored. The peak positions and weights for the unsaturated ferromagnet are shown in Table IV, and the positions and weights for the saturated ferromagnet are shown in Table V. One can see that the bandwidths and exchange splittings are, in general, reduced from the single-particle values when the full many-body theory is used, and that some of the features in Figs. 5–8 are definitely many-body satellites. In particular, the inverse photoemission density of states for the unsaturated ferromagnet (Fig. 5) has weak satellites of γ_5 symmetry (both spin orientations), while that for the saturated ferromagnet (Fig. 6) has weak satellites of minority-spin γ_5 symmetry. In the photoemission densities of states (Figs. 7 and 8), the satellite peaks are somewhat more prominent than in inverse

TABLE IV. Photoemission and inverse photoemission peaks in (crystal-symmetry-conserving) Hartree-Fock (unsaturated ferromagnet).

Symmetry	Peak energy (eV)	Peak weight
	Inverse photoemission	
h_5 (min)	0.70	1
h_5 (min)	1.40	2
h_5 (maj)	0.00	1
	Photoemission	
γ_3 (min)	0.00	2
γ_5 (min)	−1.73	3
h_3 (min)	−4.94	2
γ_3 (maj)	−0.70	2
γ_5 (maj)	−2.43	3
h_3 (maj)	−5.64	2
h_5 (maj)	−0.18	2

TABLE V. Photoemission and inverse photoemission peaks in (crystal-symmetry-conserving) Hartree-Fock (saturated ferromagnet).

Symmetry	Peak energy (eV)	Peak weight
	Inverse photoemission	
γ_3 (min)	0.00	1
h_5 (min)	0.65	1
	Photoemission	
γ_3 (min)	0.00	1
γ_5 (min)	−2.30	3
h_3 (min)	−4.94	2
γ_3 (maj)	−2.10	1
γ_3 (maj)	−1.40	1
γ_5 (maj)	−3.70	3
h_3 (maj)	−6.34	2
h_5 (maj)	−1.45	3

photoemission; majority-spin γ_5 electrons are responsible for much of the strength in the satellite peaks.

V. CONCLUSIONS

A many-body finite-cluster model of the $3d$ electrons in bcc Fe has been studied in detail. No perturbation theory was employed. This model is undoubtedly too simple to reproduce all of the rich electronic behavior of this important metal; however, it gives accurate and detailed information about some properties, and it is of general interest as an exactly soluble model which incorporates both band-structure and interaction effects on an equal footing. One fact in particular bears repeating: the competition between the two lowest-lying states (one a saturated ferromagnet, the other unsaturated with antiferromagnetic correlations) is dominated by the one-particle terms in the Hamiltonian, *not* by the Coulomb interaction. These one-particle terms depend strongly on the lattice spacing, and a recent calculation[25] has shown that fcc Fe can undergo a ferromagnetic to antiferromagnetic transition as a function of lattice spacing. Another point that cannot be addressed by effective one-particle theories such as LDA is that a strong interaction can force electrons out of states below the Fermi level and into states above it, as well as mix levels of different spin orientation.

Improvements to the model could obviously be achieved by expanding the size of the cluster. This is impractical for two reasons. The number of possible states (i.e., the size of the Hamiltonian) increases to approximately 10^8 when the cluster size is merely doubled. The increase with further expansion of the cluster is exponential. This model is only practical for very small clusters, but very useful to predict general trends. The two-atom cluster as used here can be straightforwardly applied to the ordered Fe-Co alloy.

ACKNOWLEDGMENTS

This research was supported at the Lawrence Berkeley Laboratory, by the Director, Office of Energy Research, Materials Science Division, U.S. Department of Energy, under Contract No. DE-AC03-76SF00098. One of us (E.C.S.) gratefully acknowledges support from the Shell corporation. The work was facilitated by the IBM Distributed Academic Computing Environment at the University of California, Berkeley.

[1]A. M. Oles and G. Stollhoff, Phys. Rev. B **29**, 314 (1984).
[2]J. Callaway and C. S. Wang, Phys. Rev. B **16**, 2095 (1977).
[3]K. B. Hathaway, H. J. F. Jansen, and A. J. Freeman, Phys. Rev. B **31**, 12 (1985).
[4]C. S. Wang, R. E. Prange, and V. Korenman, Phys. Rev. B **25**, 5766 (1982).
[5]R. A. Tawil and J. Callaway, Phys. Rev. B **7**, 4242 (1973).
[6]H. S. Greenside and M. A. Schlüter, Phys. Rev. B **27**, 5 (1983).
[7]E. M. Haines, V. Heine, and A. Ziegler, J. Phys. F **15**, 661 (1985); **16**, 1343 (1986).
[8]K. Lee, J. Callaway, and S. Dhar, Phys. Rev. B **30**, 1724 (1984).
[9]S. Hufner and G. K. Wertheim, Phys. Lett. **51A**, 299 (1975); C. Guillot, Y. Ballu, J. Paigne, J. Lecante, K. P. Jain, P. Thirty, R. Pinchaux, Y. Petroff, and L. M. Falicov, Phys. Rev. Lett. **39**, 1632 (1977); D. E. Eastman, F. J. Himpsel, and J. A. Knapp, *ibid.* **40**, 1514 (1978); F. J. Himpsel, J. A. Knapp, and D. E. Eastman, Phys. Rev. B **19**, 2919 (1979); L. A. Feldkamp and L. C. Davis, Phys. Rev. Lett. **43**, 151 (1979); W. Eberhardt and E. W. Plummer, Phys. Rev. B **21**, 3245 (1980); L. A. Feldkamp and L. C. Davis, *ibid.* **22**, 3644 (1980); R. Clauberg, W. Gudat, E. Kisker, E. Kuhlmann, and G. N. Rothberg, Phys. Rev. Lett. **47**, 1314 (1981); L. C. Davis, J. Appl. Phys. **59**, 25 (1986).
[10]D. R. Penn, Phys. Rev. Lett. **42**, 921 (1979); A. Liebsch, *ibid.* **43**, 1431 (1979); N. Martensson and B. Johansson, *ibid.* **45**, 482 (1980); L. C. Davis and L. A. Feldkamp, Solid State Commun. **34**, 141 (1980); A. Liebsch, Phys. Rev. B **23**, 5203 (1981); L. Kleinman and K. Mednick, *ibid.* **24**, 6880 (1981); G. Treglia, F. Ducastelle, and D. Spanjaard, J. Phys. (Paris) **43**, 34 (1982); T. Aisaka, T. Kato, and E. Haga, Phys. Rev. B **28**, 1113 (1983); R. Clauberg, *ibid.* **28**, 2561 (1983).

[11]R. H. Victora and L. M. Falicov, Phys. Rev. Lett. **55**, 1140 (1985).
[12]L. M. Falicov and R. H. Victora, Phys. Rev. B **30**, 1695 (1984).
[13]J. C. Parlebas, R. H. Victora, and L. M. Falicov, J. Phys. (Paris) **47**, 1029 (1986).
[14]A. Reich and L. M. Falicov, Phys. Rev. B **34**, 6752 (1986).
[15]J. C. Slater and G. F. Koster, Phys. Rev. **94**, 1498 (1954).
[16]V. L. Moruzzi, J. F. Janak, and A. R. Williams, *Calculated Electronic Properties of Metals* (Pergamon, New York, 1978).
[17]In this paper, the e_g representations are labeled with the subscript 3 and the t_{2g} representations are labeled with the subscript 5. These subscripts correspond to those in the character table (Table II) of the space group of the cluster.
[18]In this paper, U represents the direct on-site Coulomb integral for orbitals of the same symmetry. Other authors often use U to represent the direct on-site Coulomb integral for orbitals of *different* symmetry. We call this latter parameter U'. Atomic symmetry demands that $U'=U-2J$; our value of U is equivalent to $U'=3.5$ eV.
[19]R. H. Victora and L. M. Falicov, Phys. Rev. B **31**, 7335 (1985).
[20]C. Kittel, *Introduction to Solid State Physics*, 5th ed. (Wiley, New York, 1976), p. 465.
[21]A. W. Luehrmann, Adv. Phys. **17**, 1 (1968).
[22]Any use of the words "majority" or "minority" in the context of the spin orientation of an energy level refers to *electronic* spin, not to the spin of the hole. In particular, if the spin orientations of all the holes in the ground state are the same, these holes are in minority-spin levels.
[23]The MB-DOS should not be confused with the usual single-particle DOS; here the eigenvalues are energies of many-body states rather than single-particle excitation energies.
[24]E. Kisker, K. Schröder, W. Gudat, and M. Campagna, Phys. Rev. B **31**, 329 (1985); S. F. Alvarado, E. Kisker, and M. Campagna, Springer Proc. Phys. **14**, 52 (1986).
[25]F. J. Pinski, J. Staunton, B. L. Gyorffy, D. D. Johnson, and G. M. Stocks, Phys. Rev. Lett. **56**, 2096 (1986).